Available online at www.sciencedirect.com
ScienceDirect
Cement and Concrete Research 38 (2008) 689–698
Cement and Concrete Research

Transport properties of water and glycol in an ultra high performance fiber reinforced concrete (UHPFRC) under high tensile deformation

Jean-Philippe Charron [a,*], Emmanuel Denarié [b,1], Eugen Brühwiler [b,1]

[a] Department of Civil, Geological and Mining Engineering, École Polytechnique de Montréal, P.O. Box 6079, Montréal, Canada H3C 3A7
[b] Maintenance and Safety of Structures, Swiss Federal Institute of Technology of Lausanne, Station 18, GC B2.402, CH-1015 Lausanne, Switzerland

Received 3 July 2006; accepted 13 December 2007

Abstract

Ultra High Performance Fiber Reinforced Concretes (UHPFRC) present outstanding mechanical properties and a very low permeability. Those characteristics make them very attractive for the rehabilitation of existing structures and the conception of new structures. To define the range of admissible tensile deformation in those materials, the influence of imposed tensile deformation and subsequent cracking on permeability and absorption was studied. The transport properties of water and glycol were assessed in order to estimate the effect of the interaction of water with a specific UHPFRC. The experimental results demonstrate that permeability and absorption increase steadily until a residual tensile deformation of 0.13% is reached in the material, then water seeping rises distinctly. During experiments, the interaction of water with the UHPFRC decreases by 1 to 3 orders of magnitude the permeability and reduces absorption by approximately 50 to 85%. Test results reveal the high capability of the material to seal cracks and improve its water-tightness with time.

Keywords: Absorption; Permeability; Tensile properties; Fiber reinforcement; High performance concrete

1. Introduction

Over the last 10 years, considerable efforts to improve the deformation capacity by incorporating fibers in cementitious materials have led to the emergence of Ultra High Performance Fiber Reinforced Concretes (UHPFRC) characterized by a very low water/binder ratio and a high binder content. These new materials provide structural engineers with a unique combination of extremely low permeability, high strength, tensile strain hardening behavior, and excellent rheological properties in fresh state.

Until now, most applications of UHPFRC were dedicated to new structures [1–4] designed to take advantage of the high compressive strength and the low intrinsic permeability of those materials in an undamaged state at serviceability (mostly in prestressed structures). Another promising field of application is composite UHPFRC-concrete structures, a beam or a slab for which deteriorated concrete is replaced by UHPFRC for example [5]. Those applications are designed to withstand high levels of tensile deformation combined with very aggressive environmental loads for extended periods of time. In that context, an investigation on the influence of cracking on transport properties of water is required. Furthermore, interaction of water with UHPFRC in structures is expected to be significant and can modify the properties of the material over time. The extent of this phenomenon is still unknown.

Although in-situ conditions are different from laboratory conditions, especially when it comes to the variability of the saturation level of concrete, mechanisms suggested to explain the interaction between concrete and water in permeability and absorption tests may also explain field observations. A first mechanism used to describe water interaction in concrete is called self-sealing. It is suggested that this mechanism is related to a combination of phenomena, such as the swelling behavior

* Corresponding author. Tel.: +1 514 340 4711x3433; fax: +1 514 340 5881.
E-mail addresses: jean-philippe.charron@polymtl.ca (J.-P. Charron), Emmanuel.Denarie@epfl.ch (E. Denarié), Eugen.Bruehwiler@epfl.ch (E. Brühwiler).
[1] Tel.: +41 21 693 28 85; fax: +41 21 693 58 85.

0008-8846/$ - see front matter © 2008 Elsevier Ltd. All rights reserved.
doi:10.1016/j.cemconres.2007.12.006

of concrete under saturation, osmotic pressures, physical clogging and chemical interaction of water with the material. However, experimental evidence attributed mainly self-sealing to the chemical interaction of water with the material by causing the dissolution and deposition of soluble hydrates [6]. The second mechanism is autogenous healing. According to Edvardsen [7], it is almost solely initiated by the formation of calcium carbonate crystals ($CaCO_3$) in cracks of fractured concrete submitted to water ingress and depends largely on crack opening and water pressure. To distinguish between the latter mechanisms, one can say that localized macrocracks and access to CO_2 are required to activate autogeneous healing, whereas they are not for self-sealing. A third mechanism that results in a decrease of water penetration is the continued hydration of residual clinker [6,8].

In order to improve knowledge on water transport in UHPFRC, a research project was launched at the Swiss Federal Institute of Technology to study the permeability and the absorption of UHPFRC submitted to high tensile deformations. The objectives were to assess admissible deformations for which the material presents satisfactory transport properties and to evaluate the significance of its interaction with water.

2. Experimental details

2.1. Experimental program

UHPFRC specimens were initially submitted to a uniaxial tensile test up to a wide range of predefined levels of deformation at loading ($\varepsilon_{loading}$) as listed in the first column in Table 1. For $\varepsilon_{loading}>0.25\%$, the UHPFRC studied enters in its softening domain and a localized crack appears. The material is no longer continuous, thus the tensile deformation is rather described in terms of total displacement (Δl) measured experimentally over 100 mm. Similarly, the residual deformation after the tensile test is noted respectively $\varepsilon_{unloading}$ or $\Delta l_{unloading}$ if the loading has reached the hardening domain or the softening domain. The opening of the widest crack (w_1) created in the specimens, which was identified with a micrometric magnifying lens, is also presented in Table 1.

The unloaded specimens were then introduced in a device to estimate permeability and absorption. In order to determine the significance of the interaction of water with the UHPFRC, the transport properties of water and glycol, reactive and unreactive with cement respectively, were appraised. Glycol presents the advantage of being water-miscible and does not react with cement. Besides, its viscosity is higher than that of water [9]. Glycol is known for its capability to dissolve hydrated lime ($Ca(OH)_2$) and promotes self-sealing. Theoretically, this phenomenon should be negligible because the high amount of silica fume in the UHPFRC should consume most of the hydrated lime after many months of hydration [10]. This was confirmed by the fact that UHPFRC porosity remains unchanged after successive wetting and drying cycles made with glycol in this research. This result also demonstrates that glycol can be considered unreactive with other calcium phases of the UHPFRC cement paste.

Table 1 summarizes the experimental program and Table 2 provides the properties of permeants used in the study. The absorption capacity of specimens with a residual deformation higher than $\Delta l_{unloading}=0.33$ mm was not assessed since the presence of a wide localized crack alters test results.

Table 1
Experimental program

Tensile test		Widest crack	Permeability test[2]		Absorption test[2]	
$\varepsilon_{loading}$ or $\Delta/_{loading}$	$\varepsilon_{unloading}$ or $\Delta/_{unloading}$[1]	W_1	Water	Glycol	Water	Glycol
0%	0%	–	√	√	√	√
0.13%	0.05%	15 μm	√	√	√	√
0.25%	0.13%	35 μm	√	√	√	√
0.50 mm (0.50%)	0.33 mm	90 μm	√	√	√	√
0.75 mm (0.75%)	0.63 mm	330 μm	√	√		
1.00 mm (1.00%)	0.88 mm	520 μm	√	√		

[1]Residual tensile deformation after the tensile test.
[2]Permeability and absorption tests carried out on unloaded specimens.

Table 2
Properties of permeants at 20 °C [9]

Characteristics	Water	Glycol
Description, purity	Tap water, distilled	Ethylene glycol, 98%
CAS-number	CAS-7732-18-5	CAS-107-21-1
Chemical formula	H_2O	$HO–CH_2–CH_2–OH$
Molecular weight (g)	18.0	62.1
Molecular size (Å)	1.5	3.3
Density (kg/m^3)	998.2	1113.0
Viscosity (mPa s)	1.002	21.000
Surface tension (N/m)	7.3E−02	4.8E−02
Dielectric constant (−)	37.0	80.4

2.2. Mix design and specimen preparation

The experimental program was completed with an UHPFRC called *CEMTEC multiscale*® (Table 3) [11]. The material has a water/binder ratio of 0.14. The binder contains a cement with a high content in silicates and a low C_3A content (CEM I 52.5) and silica fume produced by precipitation (type SEPR). Others components are Fontainebleau sand and 10-mm long straight smooth steel fibers of aspect ratio equals to 50 (6% in volume).

The UHPFRC was prepared and cast horizontally in 50 x 200 x 500 mm^3 moulds. No thermal treatment was applied.

Table 3
Characteristics of the UHPFRC

Component	Content (kg/m^3)	Content (%)
Cement — CEM I 52.5	1051	39
Silica fume (d=50 mm, BET=12 m^2/g, SiO_2=93.5%)	273	10
Fontainebleau sand (d_{max}=0.5 mm)	733	27
Steel fibers (l=10 mm, d=0.2 mm, l/d=50)	468	17
Water	165	6
Superplasticizer	35	1

N.B.: Air content=4% of total volume.

Table 4
Experimental procedure

Stage of the procedure	Period (d)	Cumulative period (d)
Glycol vacuum saturation	3	3
Glycol permeability test	50	53
Drying at 60 °C	3	56
Glycol absorption test	10	66
Glycol vacuum saturation	3	69
Drying at 60 °C	3	72
Water absorption test	10	82
Water vacuum saturation	3	85
Water permeability test	50	135
Total test duration	135	135

After 3 days under sealed conditions, the specimens were removed from moulds and exposed to wet curing until 28 days. The average mechanical properties of the UHPFRC at 28 days were: f_c=168 MPa, f_t=11 MPa and E=48 GPa [12]. Moreover, the total porosity at 28 days was 4.2%, as compared to approximately 3.3% at the start of the permeability and absorption tests. The porosity was measured by the immersion method under vacuum based on the RILEM Recommendations [13]. The total porosity values are slightly higher than those measured on reactive powder concrete [14].

Afterwards, specimens were stored in a room at 20 °C and 50% relative humidity until the tensile test and subsequent core extraction were performed. The steps of the experimental procedure used to determine the transport properties are listed in Table 4. Permeability and absorption tests were completed with glycol before those with water to assess the properties on the same specimens for both permeants. As pointed out previously, glycol is considered to remain unreactive with the UHPFRC. Care was also taken to carry out absorption tests in similar conditions for both permeants. Mass loss measurements before glycol and water absorption tests have demonstrated that the fluid content of the specimens after successive glycol saturation and drying is equivalent.

2.3. Tensile strength testing and tensile behavior

Fig. 1 presents the uniaxial tensile test set-up [12] installed on a 1000 kN Schenck universal testing machine. The end parts of the prismatic specimen are glued in metallic grips specially grooved to maximize interlocking between the grip and the glue. The stress transfer from the glue to the specimen is done by adhesion. The tensile test is controlled in closed loop with the mean displacement of two LVDTs (linear variable differential transformers) fixed on both sides of the specimen. The measurement basis of the LVDTs was 100 mm and rate of displacement was 0.02 mm/min during the test.

UHPFRC specimens (prisms of 50×200×500 mm^3) were notched at mid-length to initiate cracks within the measurement basis of the LVDTs. The 20-mm deep notches on each side of the specimen reduced the cross section to 50×160 mm^2. Upon reaching a predefined level of deformation during the tensile test, the specimen was unloaded. After dismantling the specimen from the test set-up, a core of 100 mm in diameter was extracted for the permeability and absorption tests. The core was taken within the area measured by the LVDTs during the tensile test.

The tensile behavior of the UHPFRC is shown in Fig. 2a. It can be described with the next generic definition [15]. During the linear elastic phase, pre-existing microcracks in the material mainly located at the paste-aggregate interface show a slight widening. In the next strain hardening phase, some of these microcracks begin to propagate through the fiber reinforced cement paste between the aggregate to form macrocracks. Each small step in rising strength in this phase is mainly related to the strong bridging effect of fibers against the further development and opening of cracks. After reaching the maximal tensile strength, the strain softening phase starts with the development of one localized macrocrack that progressively decreases the strength. The maximal tensile strength at 28 days reached 10.8 MPa for a displacement of 0.25 mm on 100 mm (measurement basis), which correspond to $\varepsilon_{loading}$=0.25%.

Fig. 2b presents the procedure applied to UHPFRC specimens to obtain the predefined deformation with the tensile test. The specimens were damaged until the desired tensile deformation was reached and then unloaded almost completely. Afterwards, a load cycle was performed to evaluate the stiffness of the specimens. The residual deformation after unloading characterizes the modification of the UHPFRC integrity. For specimens with $\varepsilon_{unloading}$<0.13%, integrity was modified by the development of microcracks and macrocracks with an opening of w_1<35 μm (Table 1). This kind of damage has a very limited impact on water transport in the material and on its durability, as it will be demonstrated later. For specimens with $\varepsilon_{unloading}$> 0.13%, a localized macrocrack occurred with an opening wider than 35 μm.

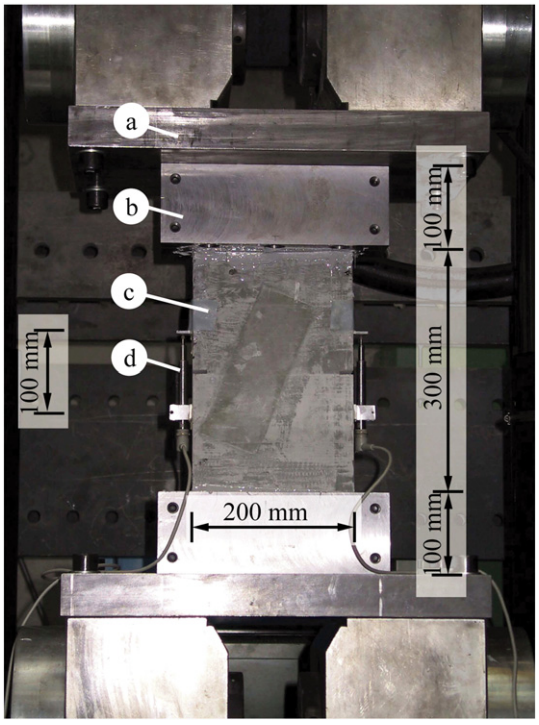

Fig. 1. Configuration of the tensile test set-up. a) base plate, b) grooved grip, c) specimen, d) linear variable differential transformer.

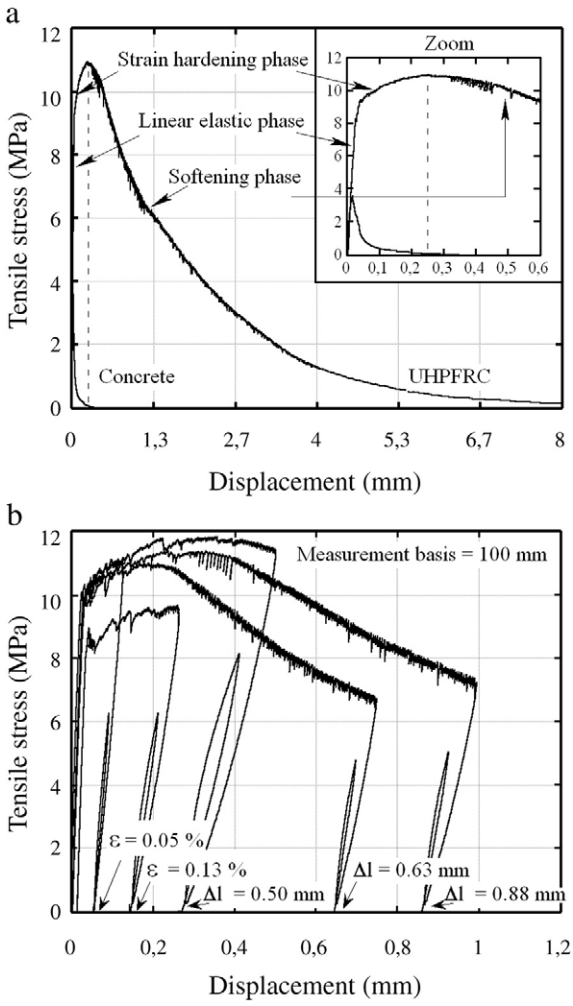

Fig. 2. Uniaxial tensile tests controlled in displacement (0.02 mm/min). a) whole tensile behavior of UHPFRC at 28 days, b) tensile test results.

2.4. Permeability testing

The liquid permeability of the UHPFRC was determined with permeability cells [16]. The device is composed of a core specimen of UHPFRC glued in an aluminum ring clamped between 2 Plexiglas tanks by threaded bars and nuts (Fig. 3). The upper tank is connected to a pipette that allows setting a specific hydrostatic pressure and evaluating the fluid flow in the specimen. The hydrostatic pressure was about 0.25 m during the experiment. The lower tank was linked to a small Plexiglas tube that allows release of liquid from the permeability cell.

Preparing the specimen consists in gluing the core specimen of UHPFRC in the aluminum ring to form a disc. Then, the disc is saturated with liquid while under vacuum for 72 h (vacuum saturation). Afterwards, the disc is clamped in the permeability cell and the tanks are filled with liquid. Considering that the specimen is saturated, the main mechanism responsible for transport is the hydrostatic pressure due to the gravity effect. Fluid flow through the specimen is periodically measured by the liquid level in the pipette. Periodically, the level of liquid is brought back to its original level to maintain a nearly constant hydrostatic pressure during the experiment. The limit of detection of the cells, which was evaluated from the accuracy of the measurement system, corresponds approximately to a permeability coefficient of 1×10^{-12} m/s.

The permeability coefficient for glycol K_g (m/s) was evaluated using Darcy's law with Eq. (1) [17], where A_p (m^2) represents the cross section of the pipette, A_s (m^2) and L_s (m) stand for the cross section and the thickness of the specimen respectively, g (m^2/s) corresponds to gravitational acceleration, h_i and h_f (m) are the hydrostatic pressure between each measurement separated by the interval of time Δt (s). In addition, the intrinsic permeability coefficient K'_g (m^2) can be calculated if the viscosity η (N s/m^2) and the density ρ (kg/m^3) of the liquid used in the test are taken into account. The intrinsic permeability coefficient evaluated with any unreactive permeant is theoretically equivalent. The last sentence is valid if the viscosity of the pore fluid and the permeant are the same. For dense cement paste this can be difficult to achieve in very thin pores. Nevertheless, in this project the fluid was seeping mainly through UHPFRC microcracks in which the fluid viscosity was most likely uniform with the permeant.

In this experimental program, permeability tests were carried out with both an unreactive permeant (glycol) and a reactive permeant (water). Because the chemical interaction between water and the UHPFRC causes a decrease of the fluid flow in the porous media, water and glycol have a different intrinsic permeability. To estimate the chemical interaction of water with the UHPFRC, a dimensionless parameter ($I_{w,p}$) was introduced in the equation of water permeability. The reduction of flow is represented here by a modification of water viscosity in the porous media. Thus, the apparent viscosity of water corresponds

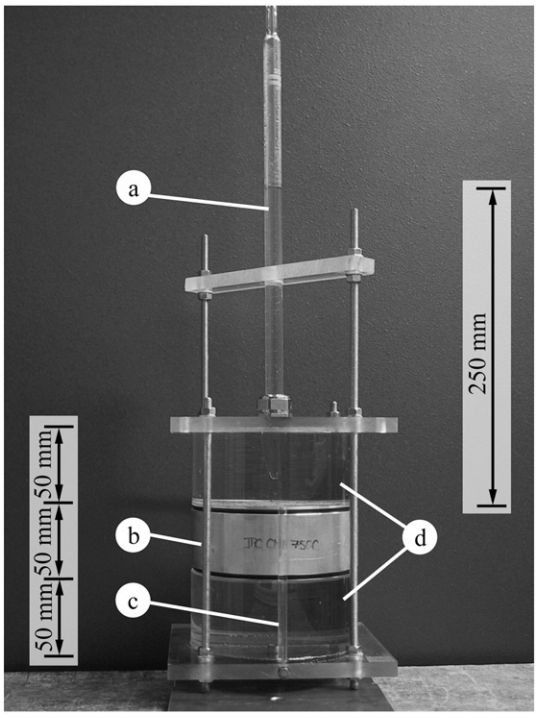

Fig. 3. Configuration of the permeability and capillarity test set-up. a) specimen glued in the aluminum ring, b) tank, c) pipette, d) tube.

to $I_{w,p} \cdot \eta_w$ as shown in Eq. (2). This procedure has no physical correspondence; in reality, there is no change in viscosity. Combining the latter equations, this procedure allows the estimation of the interaction parameter $I_{w,p}$ with water and glycol permeability results (Eq. (3)). Note that in Eqs. (1)–(3), subscript "$_w$" stands for water and "$_g$" for glycol.

$$K_g' = K_g \cdot \left(\frac{\eta_g}{\rho_g g}\right) = \left(\frac{A_p L_s}{A_s \Delta t} \cdot \ln\frac{h_i}{h_f}\right) \cdot \left(\frac{\eta_g}{\rho_g g}\right) \quad (1)$$

$$K_w' = K_w \cdot \left(\frac{I_{w,p}\eta_w}{\rho_w g}\right) = \left(\frac{A_p L_s}{A_s \Delta t} \cdot \ln\frac{h_i}{h_f}\right) \cdot \left(\frac{I_{w,p}\eta_w}{\rho_w g}\right) \quad (2)$$

$$I_{w,p} = \left(\frac{K_g}{K_w}\right) \cdot \left(\frac{\eta_g}{\eta_w} \cdot \frac{\rho_w}{\rho_g}\right). \quad (3)$$

Moreover, the theoretical estimation of glycol permeability coefficients from the crack opening of UHPFRC specimens was derived from the Hagen–Poiseuille law (Eq. (4)) [18]. The fluid flow in damaged specimens depends mainly on crack characteristics in terms of length l (m), roughness of surface ξ (dimensionless) and opening w (m). While the permeability coefficient is proportionate to the cube of the crack opening, utilization of the characteristics of the widest crack (l_1 and w_1) measured on specimens is sufficient to obtain an adequate estimation of permeability [17].

$$K'_{g,\text{th}} = \frac{\xi \cdot l_1 \cdot w_1^3}{12 \cdot A_s} \cdot \left(\frac{\rho_g g}{\eta_g}\right). \quad (4)$$

2.5. Absorption testing

The absorption test is carried out with the device described previously in the permeability testing section. However, the specimen preparation is different. Specimens are dried for 72 h at 60 °C instead of being vacuum-saturated, and the inferior tank is kept empty. The oven temperature (60 °C) was limited to avoid any additional microcracking due to drying and to reduce the activation of hydration of the residual clinker in the specimen.

The main mechanisms responsible for fluid transport during the absorption test are hydrostatic pressure due to the gravity effect and capillary suction. If the head pressure (ρgh) remains constant (depth of penetration of the liquid in the material is negligible), the average flow can be estimated using Eq. (5). The equation is based on Poiseuille's law [19] where the pressure in the fluid is evaluated with Laplace's law. As shown, fluid penetration depends mainly on the characteristic pore radius r_c (m), the properties of the fluid and the contact angle θ between the meniscus and the pore surface. The left-hand side in brackets represents the capillary suction and the right-hand side in brackets corresponds to the head pressure force (h=0.25 m).

$$V(t) = A_c \cdot \sqrt{\left[\frac{1}{2\eta}\left(r_c \cdot \sigma \cdot \cos\theta + \frac{r_c^2 \cdot \rho g h}{2}\right)\right] \cdot t}. \quad (5)$$

The significance of each force in the fluid flow depends on the pore radius. For r_c<40 μm, the capillary suction is predominant, whereas head pressure is the most significant for r_c>140 μm. Between those values, the effect of both forces are of the same magnitude.

Absorption tests are commonly interpreted via sorptivity S (l/m^2 s$^{0.5}$), which represents the absorbed volume of liquid divided by the area of specimen and square root of time. Sosoro [20] also suggested Eq. (6) to estimate the sorptivity of an unreactive liquid (here glycol) from the pore structure C (dimensionless), the effective porosity of the material accessible to liquid P_{eff} (dimensionless) and the properties of the liquid. As in the previous section, the interaction between water and concrete is taken into account by introducing parameter $I_{w.a}$ used to describe the apparent viscosity (Eq. (7)). The interaction parameter $I_{w.a}$ is estimated with the combination of water and glycol absorption results in Eq. (8). The effective porosity reached by the two permeants in the UHPFRC ($P_{\text{eff, }g}$ and $P_{\text{eff, }w}$) can be considered equivalent because surface tension has a minor impact on pore saturation in a material with small pores [21]. Moreover, experimental results on concrete have demonstrated a close value for the effective porosity reached by water and glycol [22].

$$S_g = \sqrt{2 \cdot C \cdot P_{\text{eff},g} \cdot \frac{\sigma_g}{\eta_g}} = \frac{\Delta V_g}{\sqrt{\Delta t}} \quad (6)$$

$$S_w = \sqrt{2 \cdot C \cdot P_{\text{eff},w} \cdot \frac{\sigma_w}{I_{w,a}\eta_w}} = \frac{\Delta V_w}{\sqrt{\Delta t}} \quad (7)$$

$$I_{w,a} = \left(\frac{S_g^2}{S_w^2}\right) \cdot \left(\frac{\eta_g}{\eta_w} \cdot \frac{\sigma_w}{\sigma_g}\right). \quad (8)$$

3. Results

3.1. Permeability testing

The evolution of permeability coefficients over time for various levels of residual tensile deformation in the UHPFRC is illustrated in Fig. 4 for glycol and water. For each testing condition, the average curve obtained for three specimens is shown. The shape of the permeability curves indicates a nonlinear behavior during the first 14 days of the experiments. Afterwards, the permeability coefficients become nearly constant, showing that a steady flow of liquid seeps through the material.

Water and glycol test results demonstrate that permeability increases with the level of tensile deformation applied to the UHPFRC (Fig. 4). Test results show a gradual increase in permeability until a tensile deformation at unloading of 0.13% is reached. Then, permeability rises significantly. This characteristic value of deformation corresponds to a cumulated crack opening of 0.13 mm considering the measurement basis of 100 mm of the tensile test. One can also observe that water permeability increases softly with the level of damage compared to glycol permeability. Moreover, water penetrates less in the UHPFRC, with permeability coefficients 1 to 2 orders of

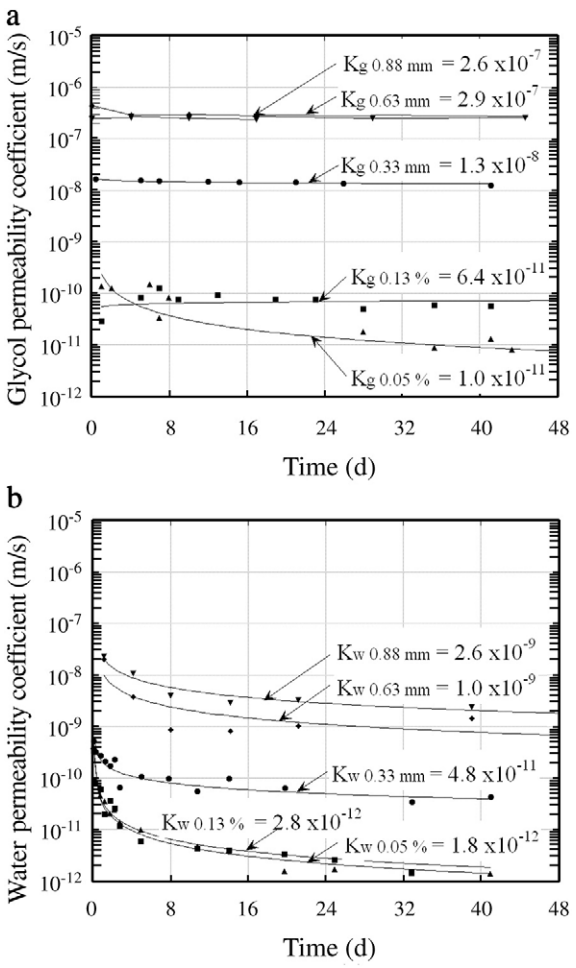

Fig. 4. Permeability coefficient of strained UHPFRC. a) for glycol, b) for water.

magnitude lower than those of glycol. This feature will be further explained in the Discussion.

In order to verify the relationship between the crack opening in the UHPFRC and permeability, experimental results where plotted with the theoretical estimation of glycol permeability according to the Hagen–Poiseuille law (Eq. (4)). With the interaction between water and UHPFRC being significant, the analysis did not use water permeability results. The dimensionless parameter ξ representing surface roughness was fitted to obtain the best correlation between experimental and theoretical glycol permeability coefficients. When surface roughness is significant, as likely in UHPFRC, ξ becomes low to describe the difficulty with which the fluid flows through the material. The theoretical estimation shown in Fig. 5 was obtained with $\xi = 9.1 \times 10^{-4}$. Gérard [23] reported surface roughness values ranging from 1.1×10^{-1} to 1.6×10^{-1} for concrete damaged with tensile tests and 1.0×10^{-2} to 9.0×10^{-2} for concrete damaged with bending tests. Thus, the value obtained in the present study is very small.

Fig. 5 shows a good correlation between experimental results and theoretical estimation of permeability in relation to the opening of wider cracks within the specimens. This observation is consistent with test results presented recently [18,24].

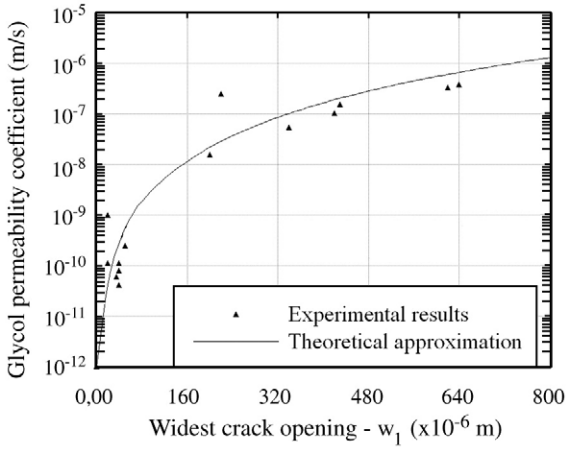

Fig. 5. Theoretical and experimental glycol permeability coefficient of strained UHPFRC.

3.2. Absorption testing

The water and glycol absorbed by specimens is presented in Fig. 6 as a function of the square root of time. The curves correspond to the average results obtained for three specimens.

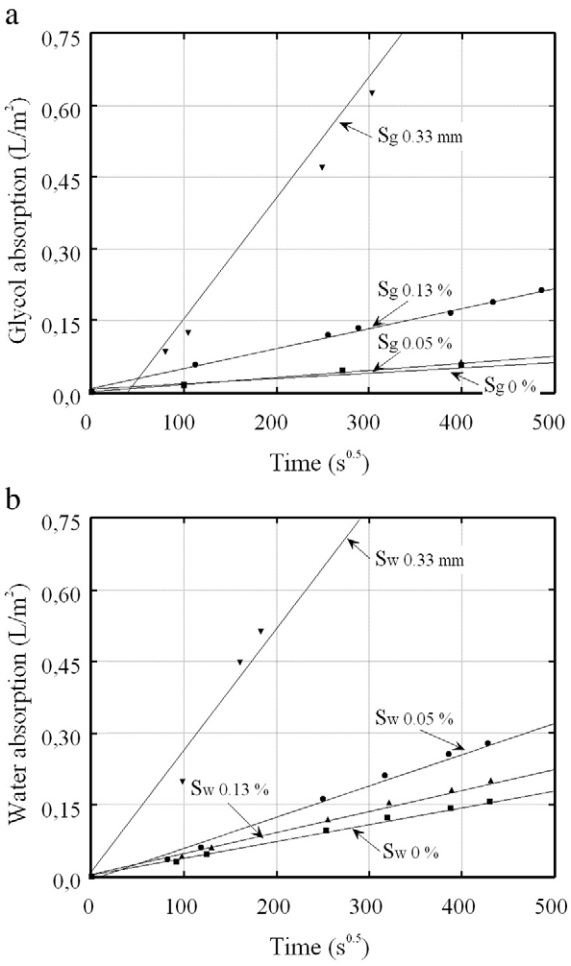

Fig. 6. Absorption results of strained UHPFRC. a) for glycol, b) for water.

Table 5
Interaction parameters between water and strained UHPFRC

Tensile test	Permeability test(1)			Absorption test(2)		
$\varepsilon_{unloading}$ or $\Delta l_{unloading}$	K_g (m/s)	K_w (m/s)	$I_{w,p}$ (−)	S_g (L/m^2 s$^{0.5}$)	S_w (L/m^2 s$^{0.5}$)	$I_{w,a}$ (−)
0%	–(3)	–(3)	–	0.000114	0.000353	3.3
0.05%	1.00E−11	1.80E−12	104.8	0.000150	0.000442	3.6
0.13%	6.40E−11	2.80E−12	431.3	0.000426	0.000656	13.4
0.33 mm	1.30E−08	4.80E−11	5110.1	0.002740	0.002519	37.4
0.63 mm	2.90E−07	1.00E−09	5471.7	–	–	–
0.88 mm	2.60E−07	2.60E−09	1886.8	–	–	–

(1): Permeability coefficient evaluated between the 35th and the 45th day of the permeability test.
(2): Sorptivity evaluated from the beginning to the 3rd day of the absorption test.
(3): Permeability measurements fall under the detection threshold of the testing device.

Absorption of water in conventional concrete generally shows a rapid kinetic at the beginning and a subsequent constant flow rate. For undamaged UHPFRC specimens ($S_{0\%}$), one can observe a linear curve of absorption from the beginning of the experiment. The trend is also noted for specimens with residual deformation, but is less obvious for the highest level of deformation ($S_{0.33\ mm}$).

Test results indicate that absorption of glycol and water increases with the level of residual deformation in UHPFRC specimens. Liquid absorption is also generally higher with water. Besides, the amount of water absorbed by undamaged specimens of UHPFRC is similar to the one measured in reactive powder concrete [25].

3.3. Interaction between water and the UHPFRC

Table 5 summarizes the experimental results obtained during the project. Permeability and sorptivity coefficients for glycol and water are listed for levels of residual tensile deformation studied. The comparison of glycol and water penetration in specimens permits to estimate the magnitude of the interaction of water with UHPFRC considering the properties of permeants and that glycol remains unreactive.

The interaction factors calculated with permeability tests increase clearly with the level of damage in specimens. Only one value obtained for 0.88 mm of deformation does not follow the trend (this will be explained in the next section). The interaction factors estimated with absorption tests also increase with damage; however the magnitude of the values is lower than for permeability tests.

4. Discussion

4.1. Permeability testing

As expected, permeability results indicate that the fluid flow in the UHPFRC rises with increasing the level of damage of the material. The abrupt increase of fluid flow observed between $\varepsilon_{unloading}=0.13\%$ and $\Delta l_{unloading}=0.33$ mm is related to the presence of a localized macrocrack in the UHPFRC for the latter deformation. Indeed, $\Delta l_{unloading}=0.33$ mm was produced by a deformation at loading of 0.50% (Table 1), which is well above the average tensile deformation required to activate the opening of a localized macrocrack for this material ($\varepsilon_{t\ localization}=0.25\%$, Fig. 2).

Previous studies have also reported a rise in permeability with increasing macrocrack opening in concrete [26,27]. In those studies, a cumulated crack opening of 0.05 mm at unloading was needed to note a clear enhancement of permeability. This value is three times below the one estimated for the UHPFRC. The higher deformation capacity of the UHPFRC before the modification of the fluid ingress is thus obvious. In fact, this is related to the crack pattern that develops in each material. For a similar level of deformation, multiple macrocracks with relatively small openings will appear in the UHPFRC, as opposed to fewer macrocracks with relatively large openings developing in conventional concrete. Since permeability rises proportionally to the cube of the crack width, several narrow macrocracks are less permeable than one wide macrocrack.

One can also observe that the water permeability curves stabilized much more slowly than those of glycol at the beginning of the test. This phenomenon is probably due to the rapid chemical interaction of water with the material.

Concerning the comparison of experimental and theoretical estimation of permeability, the best approximation was obtained with a relative low value of $\xi=9.1\times10^{-4}$ compared to expectations for conventional concrete. Since this parameter is inversely proportional to the surface roughness, the value indicates that the path followed by water in the cracks is very complex and consequently long. This is most probably due to the presence of multi-branching cracks in the UHPFRC.

4.2. Absorption testing

Absorption measurements on conventional concrete generally show curves with two slopes. The rate of absorption is high at first and then decreases. As observed in [14], the experimental results for undamaged UHPFRC specimens show only a constant rate of absorption. This difference is related to the limited amount of capillary pores in UHPFRC [14]. The trend is also noted for specimens with residual deformation, but is less obvious for the highest level of deformation ($S_{0.33\ mm}$). In that case, the localized macrocrack within the specimens represents a large artificial capillary pore and increases greatly the absorption capacity of the material.

Test results in Fig. 6 indicate that absorption of glycol and water increases with the level of residual deformation in UHPFRC specimens. Few results are available in the literature on the influence of damage on capillary absorption. Lunk [28] showed an increase in capillary absorption in unsaturated concrete for thinner cracks. The divergence of results with this paper is probably associated with the differences in the range of crack openings studied and the experimental technique used in the projects. Liquid absorption described in this paper is initiated by the combination of hydrostatic force and capillary suction, instead of solely capillary suction in Lunk's work.

Furthermore, multiple macrocracks with various openings are present in an UHPFRC specimen. For macrocracks wider than 40 μm, the hydrostatic force produced by the head pressure of liquid partly or totally controls the absorption in the crack (see Section 2.5, Eq. (5)). However, capillary suction is predominant in macrocracks and pores narrower than 40 μm on the same specimen. On the whole, the hydrostatic force has probably played a significant role in fluid transport mechanism in UHPFRC and may explain the greater absorption rate for a higher range of residual deformation. Moreover, the wider fracture process zone of the UHPFRC compared to concrete, which is favorable to absorption, may also explain the trend of the results.

During absorption tests, water has seeped more than glycol in the UHPFRC. In fact, surface tension and viscosity of water are favorable to measure higher absorption. The analysis in the next section will however demonstrate that absorption of water should be higher if interaction between water and UHPFRC was negligible as likely with glycol.

Besides, it was pointed out previously that permeability rises distinctly when residual deformation exceeds $\varepsilon_{unloading}=0.13\%$. Absorption measurements also show a clear enhancement of fluid penetration under the same conditions. The existence of a localized macrocrack in the UHPFRC at $\Delta l_{unloading}=0.33$ m results in an increase in both the absorption and permeability of liquid.

4.3. Interaction between water and the UHPFRC

It should be reminded that interaction is interpreted here as a modification of the viscosity of water in the UHPFRC. A short-term interaction ($I_{w,a}$) is evaluated from the absorption tests and a mid-term interaction ($I_{w,p}$) is estimated from permeability tests. The interaction parameters calculated with Eqs. (3) and (8) are also given in Table 5.

Since the short-term and mid-term interactions rise with increasing the level of damage in the UHPFRC, the interaction is favored by the presence of cracks and their opening. However, the interaction should logically decrease after reaching an optimum, because for an infinite crack the surface effects on water penetration become negligible. This probably explains the reduction of the interaction parameter calculated for $\Delta l_{unloading}>0.63$ mm in permeability tests.

On the other hand, the interaction of water with the UHPFRC is greater during permeability tests than during the absorption tests. Considering the properties of permeants, water permeability should be 2 to 3 orders of magnitude higher if water was moving freely like glycol in the UHPFRC. Similarly, water absorption represents about 15 to 50% of expectations if negligible interaction was occurring as with glycol. The latter estimations are obtained by using interaction parameters equal to 1 in Eqs. (3) and (8). Longer exposure to water also promotes more interaction because the parameters are higher in permeability tests. Consequently, the interaction between UHPFRC and water must be related at least partly to gradual mechanisms, unless different mechanisms are responsible for short-term and long-term interactions.

The identification of the mechanisms responsible for the interaction of water in the UHPFRC is not obvious. Concerning the self-sealing associated with the dissolution and the deposition of soluble hydrates, one could say that a very small amount of hydrated lime can precipitate in the porous network due to its previous consumption by silica fumes, but other phases can. Besides, autogeneous healing is certainly active in UHPFRC. The healing generally attributed to calcium carbonate precipitation in cracks can also be due to the hydration of residual clinker at crack surface. Results reported in [8] show that residual clinker grains exposed on the surface of a crack reacts with water within a few minutes. Consequently, hydration products slow down further water penetration in cracks. The rapidity with which the reaction occurs is consistent with the interaction noted during absorption tests. Finally, the mechanism of continued hydration in areas where the material is undamaged can also decrease water transport over time.

Although the role played by each mechanism cannot be assessed, it is clear that the chemical interaction of water progressively improves the tightness of the UHPFRC. Depending on how significant the continued hydration of residual clinker is in the interaction process, mechanical properties of the material are expected to increase with time (mechanical strength is proportionate to the degree of hydration). The utilization of strained UHPFRC at serviceability will promote such process. Consequently, strained UHPFRC could present in the long term equivalent properties to those of unstrained material. As a matter of fact, recent research projects have illustrated such phenomenon. Parant [29] has shown that UHPFRC specimens subjected to fatigue tests and then immersed in water with chlorides exhibit a greater flexural resistance in comparison to control specimens. Pimienta et al. [30] have also reported that the flexural strength of pre-cracked UHPFRC specimens remains unchanged after three months under severe conditions. Self-healing was suggested as an explanation for this latter observation. Finally, self-healing phenomenon was demonstrated by Ying-Zi et al. [31] in Engineered Cementitious Composites (ECC). According to the authors, self-healing performance depends on the cracking properties of the matrix adjacent to the damaged area and the seal-healing capability of the material. In this context, UHPFRC has the characteristics for presenting significant self-healing capability since its matrix is very dense and a large amount of residual clinker is available to hydrate and seal cracks.

5. Conclusions

The objectives of the research project were to assess the permeability and the absorption of UHPFRC for two permeants, water and glycol, and to evaluate the significance of its interaction with water. Analysis of experimental results has shown:

1. The optimized fibrous reinforcement of the UHPFRC allows achieving a noteworthy tensile strain hardening up to 0.25% on notched specimens, where the maximal tensile strength (10.8 MPa) is reached. Until that level of deformation is reached, UHPFRC integrity is only modified by the

development of microcracks and macrocracks thinner than 50 μm, then the material starts to display its softening behavior.

2. Penetration of liquid in terms of permeability and absorption coefficients increases steadily until a residual tensile deformation of 0.13% is reached in UHPFRC. As a basis of comparison, at this threshold value, the water permeability of UHPFRC ($K_w \leq 4.8 \times 10^{-11}$ m/s) is lower than that of an uncracked concrete with a water/binder ratio equal to 0.45 [27].
3. The utilization of glycol and water as permeants, unreactive and reactive with residual clinker respectively, has permitted to evaluate the interaction of water with UHPFRC during the experiments. It was observed that permeability and absorption of water are lower to what could be anticipated if water was moving freely in the material. Hence, the combined effects of self-sealing, self-healing and continued hydration, which are expected to occur with water, reduce absorption by approximately 50 to 85% after 3 days and decrease permeability by 2 to 3 orders of magnitude after 40 days. The interaction phenomenon is thus quite significant.
4. From previous conclusions, in spite of the application of very high tensile deformations, the UHPFRC shows a high capability to seal micro and macrocracks and to improve its water-tightness when exposed to water. It follows for practical consideration that water-tightness or very low permeability is preserved for strained UHPFRC in structures at serviceability. Based on the experimental results, limits of tensile deformation for the UHPFRC under study were suggested according to environmental conditions [16].

Besides, further research is required to estimate the impact of key factors concerning water flow in UHPFRC. It is expected that water interaction depends on crack patterns created in the UHPFRC, type of loading, material maturity and environmental conditions. Moreover, chloride penetration in UHPFRC and water interaction to consider in long-term predictions has to be assessed.

Acknowledgments

This project was financially supported by the Swiss State Secretariat for Education and Research (SER) and the Fonds pour la Formation de Chercheurs et l'Aide à la Recherche (FCAR) of the Québec government, in the context of the European project Sustainable and Advanced Materials for Road Infrastructures (SAMARIS). Research was carried out during the postdoctoral project of the first author at the Swiss Federal Institute of Technology in Lausanne.

References

[1] P.C. Aïtcin, M. Lachemi, R. Adeline, P. Richard, The Sherbrooke reactive powder concrete footbridge, Structural Engineering International IIABSE 8 (2) (1998) 140–144.
[2] A. Bekeart, M. Behloul, J. Dugat, R. Adeline, H. Lacombe, EDF plant of Cattenom — reactive powder concrete for nuclear applications, Travaux 752 (1999) 69–72 (*Original in French*).
[3] Y. Tanaka, H. Musya, A. Ootake, Y. Shimoyama, O. Kaneko, Design and construction of Sakata–Mirai footbridge using reactive powder concrete, Proceedings of the 1st FIB Congress, Osaka, Japan, 2002, pp. 417–424.
[4] M. Behloul, K.C. Lee, Ductal Seonyu footbridge, Structural Concrete 4 (4) (2003) 195–201.
[5] E. Denarié, Structural rehabilitations with ultra-high performance fibre reinforced concretes (UHPFRC), in: M. Alexander, H.-D. Beushausen, F. Dehn, P. Moyo (Eds.), International Conference on Concrete repair, rehabilitation and retrofitting, Taylor & Francis, London, 2005.
[6] N. Hearn, Self-sealing, autogenous healing and continued hydration: what is the difference? Materials and Structures 31 (1998) 563–567.
[7] C. Edvardsen, Water permeability and autogenous healing of cracks in concrete, ACI Materials Journal 96 (4) (1999) 448–454.
[8] C. Hall, W.D. Hoff, S.C. Taylor, M.A. Wilson, B.-G. Yoon, H.-W. Reinhardt, M. Sosoro, P. Meredith, A.M. Donald, Water anomaly in capillary liquid absorption by cement-based materials, Journal of Materials Science Letters 14 (1995) 1178–1181.
[9] J.A. Dean, Lange's handbook of chemistry, McGraw-Hill, Montreal, 1999.
[10] M. Cheyrezy, V. Maret, L. Frouin, Microstructural analysis of RPC (reactive powder concrete), Cement and Concrete Research 25 (7) (1995) 1491–1500.
[11] P. Rossi, E. Parant, O. Laurence, P. Fakri, A. Arca, Mechanical behavior of a new cementitious composite with strain hardening, Bulletin des Laboratoires des Ponts et Chaussées 238 (2002) 25–38 (*Original in French*).
[12] K. Habel, Structural behavior of composite elements combining ultra-high performance fiber reinforced concretes (UHPFRC) and reinforced concrete, Ph.D. thesis of the Switzerland Technical Institute of Technology, Switzerland, 2004.
[13] RILEM TC 14-CPC, CPC 11.3 Absorption of water by immersion under vacuum, Materials and Structures 17 (1984) 391–394.
[14] N. Roux, C. Andrade, M.A. Sanjuan, Experimental study on reactive powder concrete durability, Annales de l'Institut technique du bâtiment et des travaux publics 532 (1995) 133–141 (*Original in French*).
[15] Y.V. Zaitsev, Inelastic properties of solids with random cracks, in: Z.P. Bažant (Ed.), Proceedings of the William Prager Symposium on Mechanics of geomaterials: rocks, concrete, soils, John Wiley & Sons, Evanston, U.S.A., 1985, pp. 89–128.
[16] J.-P. Charron, E. Denarié, E. Brühwiler, Permeability of UHPFRC under high stresses, Materials and Structures (in press), doi:10.1617/s11527-006-9105-0.
[17] H.W. Reinhardt, N. Hearn, M. Sosoro, Transport properties of concrete, in: H.W. Reinhardt (Ed.), RILEM Report 16 - Penetration and permeability of concrete, Stuttgart, Germany, 1997, pp. 213–264.
[18] V. Picandet, Influence of a mechanical damage on water permeability and diffusivity of concrete, Ph.D. thesis of Université de Nantes, France, 2001. *Original in French.*
[19] L. Merouani, Sorption and humidity transfer phenomena in building materials, Ph.D. thesis of Institut National Polytechnique de Grenoble, France, 1987. *Original in French.*
[20] M. Sosoro, Immiscible liquids: unsaturated displacement, in: H.W. Reinhardt (Ed.), RILEM Report 16 - Penetration and permeability of concrete, Stuttgart, Germany, 1997, pp. 82–93.
[21] M. Sosoro, Transport of organic fluids through concrete, Materials and Structures 31 (1998) 162–169.
[22] M. Sosoro, Liquid displacement in concrete by capillary forces, Otto Graf Journal 6 (1995) 11–34.
[23] B. Gérard, Study on mechanical-chemical coupling for the long term durability of structures for stockpiling of nuclear waste, Ph.D. thesis of Ecole Normale Supérieure de Cachan, France, 1996. *Original in French.*
[24] H.W. Reinhardt, M. Jooss, Permeability and self-healing of cracked concrete as a function of temperature and crack width, Cement and Concrete Research 33 (2003) 981–985.
[25] M. Cheyrezy, Improvement of durability and water tightness of concrete structures by use of high and ultra high performance concrete, SIA Documentation D0702 (1995) 93–97 (*Original in French*).
[26] K. Wang, D.C. Jansen, S.P. Shah, A.F. Karr, Permeability study of cracked concrete, Cement and Concrete Research 27 (3) (1997) 433–439.

[27] C.W. Aldea, S.P. Shah, A.F. Karr, Permeability of cracked concrete, Materials and Structures 32 (219) (1999) 370–376.
[28] P. Lunk, T. Müller, F.H. Wittmann, Moisture and ion transport in cracked reinforced concrete members, Highway Federal Office of Switzerland, Report, vol. 538, 1998, (*Original in German*).
[29] E. Parant, Damage mechanisms and mechanical behaviors of a multi-scale under harsh conditions: fatigue, impact, corrosion, Ph.D. thesis of Ecole Nationale des Ponts et Chaussées, France, 2003. *Original in French.*
[30] P. Pimienta, G. Chanvillard, Retention of the mechanical performance of ductal specimens kept in various aggressive environments, FIB Symposium Concrete Structures: Challenge of Creativity, Avignon, France, 2004, pp. 24–28.
[31] Y. Ying-Zi, M.D. Lepech, V.C. Li, Self-healing of engineered cementitious composites under cyclic wetting and drying, International Workshop on Durability of reinforced Concrete under Combined Mechanical and Climatic Loads, Qingdao, China, 2005, pp. 231–242.